# Experimental study of the void-fraction distribution in a bisectional bubble-column reactor

Andrej Bombač

**Abstract:**
This paper presents the distribution of the local void fraction (LVF) in a pilot bisectional bubble-column reactor with a diameter of 0.63 m, where the two-phase mixing of air and water was performed with a static mixer. Because of the lack of such data in the literature, the LVF was measured at 342 nodes in the vertical half-section plane of the column. Detecting the phases at a particular point with a resistivity probe and then a further phase-discrimination procedure using the probe signal enabled a quantitative evaluation of the reactor. Small differences between the volume-integrated LVF values and the gas-holdup measurements based on a liquid-height changes showed reasonably good agreement under all conditions.

**Keywords:**
bisectional bubble-column, resistivity probe, local void fraction, integral void fraction, gas holdup.

## 1 Introduction

A bisectional reactor is formed from two sections, i.e., the bottom section, where the two-phase mixing must be ensured, and the upper section, through which the mixture of the aqueous medium and the oxygen gas flows [1,2]. Between these two sections, a separator is located, which allows limited mass transfer based on the limited transfer of the momentum of the rising gas–liquid mixture. As an alternative to conventional impeller stirring, efficient mixing can be ensured by introducing the two-phase mixture at the reactor inlet with a static mixer. The two-phase mixture is prepared in an external loop, whereas the aqueous phase is maintained by a pump, and the reactor feed can also be introduced through this loop.

With bubble-column reactors most of the studies were focused on the global parameters, for example, gas holdup, mass-transfer rate, or pressure drop, and only a few studies present the void-fraction distributions (VFDs). As reported by Krepper et al. [3], the dispersed gas preferentially flows centrally in the bubble column, which leads to an uneven VFD, setting up a global circulation pattern that is basically density-driven. So, the VFDs are of great interest and were extensively studied in various gas–liquid contactors [4–6], in cylindrical bubble columns [7] and with a special emphasis on the flow symmetry [8]. Owing to the increased interest in industrial devices of various shapes, such as rectangular and square bubble columns, VFD studies can be found in [3].

**Assist. Prof. Andrej Bombač**, PhD., University of Ljubljana, Faculty of Mechanical Engineering

The LVF can be determined experimentally using any physical principle where the liquid and gas behave differently. The first measurements of the LVF were made by measuring the volume of separated air taken away from a two-phase sample (i.e., the vacuum-sampling technique). Later modifications that involve introducing a pair of impedance probes [9], or two pairs of LED/photo detectors [10,11], significantly improved the LVF and bubble-size measurements. The impedance probes based on resistivity changes (i.e., an R probe) in the gas or liquid phase were, because of the simple probe and circuitry, and the low costs [12], extensively used in a variety of systems [5,13,14]. In accordance with the demands for robustness, a very fast response to the phase change is achieved with a very small diameter of approximately 10–50 μm, which also enables the detection of very small bubbles. Based on a literature survey, it is clear that R probes were used in various multi-phase systems to determine the void fraction in bubble columns [3,13], large diameter channels [15] and aerated stirred tanks [5,14,16].

In this study the focus is on the VFD in the bottom section of a pilot bisectional bubble-column reactor using an external loop. The LVF measurements were made with an R probe, which ensured insensitivity to the flow direction with a large angle of attack (less than 90°) and enabled reasonable accuracy and reproducibility for 342 nodes in the vertical half-section plane of the column for each hydrodynamic regime. Three different hydrodynamic regimes with varying liquid- and air-flow rates were observed. The LVF values were based

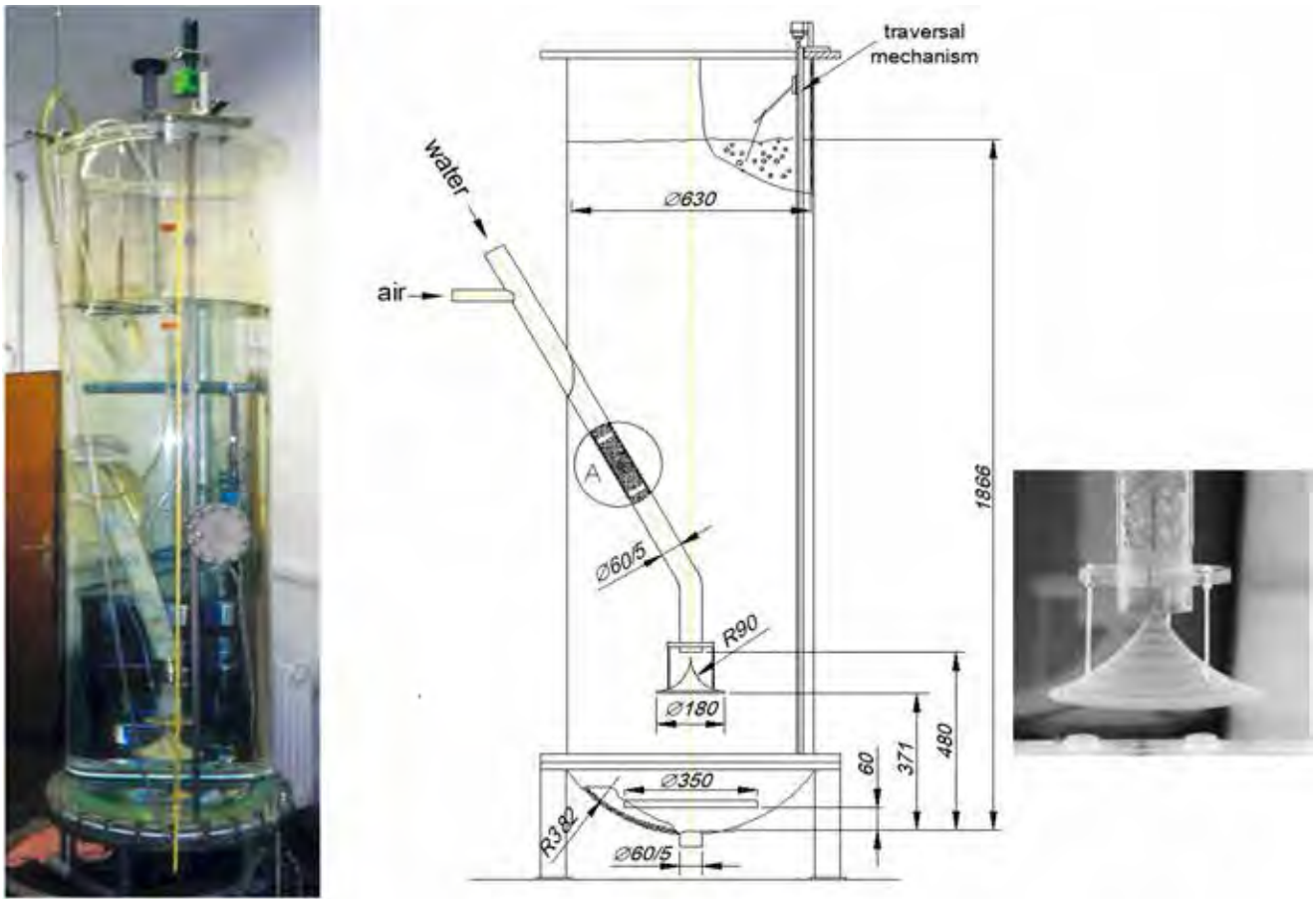


***Figure 1 :*** *Bubble column with its geometrical parameters and the deflector detail.*

on a phase-discrimination procedure using a single threshold. The spatial distributions of the void fraction, radially and based on volume-integrated values of the LVF, are presented and compared for each hydrodynamic regime. The influence of the bubble buoyancy, acting upwards on the free surface, can be recognized from the contours of the LVF in all the regimes. As well as the areas with a remarkably high gas-phase concentration, the two-phase circulation loops can also be recognized from the peaks of the LVF when it is radially integrated.

## 2 Experimental technique

The void-fraction measurements were performed in a cylindrical bisectional bubble column made of transparent polycarbonate material. It consisted of two parts: (a) an upper cylindrical vessel of inner diameter 630 mm, wall thickness 10 mm and height of 2220 mm, and (b) a rounded bottom of 383 mm in diameter and the same wall thickness. For the probe positioning in the vertical *r–z* plane, a special traversal mechanism was mounted on the inner vessel wall, as can be seen in *Fig.1.* On the opposite side in the same vertical plane, a static mixer with a centrically positioned downward-oriented outlet was placed. To redirect the axial outgoing two-phase flow from the static mixer to the radial flow, a curved conical deflector was installed. To prevent even single bubbles from entering the outlet and the liquid pump, a plate was placed at the vessel bottom, with a thin gap of 16 mm between the plate edge and the bottom wall. A two-phase mixture of air and water was produced with a Sulzer SMV–12 static mixer, made of a polycarbonate tube with an inner diameter of 50 mm, filled with static mixing packages. The liquid-level height in the column was at $H$ = 1866 mm. A Grundfos TYP CRNE 16 water pump ensured a constant water flow rate, automatically controlled by a preset. To prevent water heating in the column due to the pump's operation, the water temperature was controlled and kept constant at 22 ±0.5 °C. This was enabled by exchanging the proper quantity of water with colder water (14 °C) from a water basin with a volume of 12 $m^3$ in the basement below the lab. An Enders–Hauser electromagnetic flow meter of type Promag-F with a relative error of ±0.5 % of the reading was used for the volumetric water flow-rate measurements. Furthermore, the volumetric air flow rate was adjusted with a precision needle valve and measured by a TG 300 MLW calibrated rotameter with an accuracy class of 2 and corrected for the pressure head. A Greisinger GDH 07 pressure gauge and

thermocouple were installed inline to correct the flow-meter readings as follows:

$$Q = Q_{\text{read}}\sqrt{\frac{p}{p_0}\cdot\frac{T_0}{T}} \quad (1)$$

where $Q$ represents the corrected volumetric flow rate, $Q_{read}$ is the flow-meter reading, $p$ is the pressure, and $T$ is the temperature. The pressure and temperature calibration constants refer to $p_0$ and $T_0$, respectively, and were given by the manufacturer. The experimental setup is shown in *Fig.2*. The gas holdup ($\alpha_G$) in the column was measured with an improved three-point "level taker". This comes originally from the liquid-level height measurements at the column wall, but with a very high deviation due to liquid waving. The three-point level taker successfully damped the liquid-level oscillation in the glass measuring cylinder. The global gas holdup was defined as:

$$\alpha_G = 100(H_g - H)/H_g, \quad (\%) \quad (2)$$

where $Hg$ denotes the level height by gassing, and $H$ denotes the level without. The relative reproducibility error for each hydrodynamic regime was less than 5 %, averaged over at least 20 gas-holdup measurements. Some previous experimental studies of the LVF distribution based on R-probe response measurements were presented for different systems, i.e., in a bubble column [12] using the closing-valve technique for the calibration of the discrimination procedures or using gassed stirred vessels [14,17], where the repeatability error of the local void fraction was found to be within 2.3% (with an angle of attack of less than 90°) and 10% (for angles ranging between 90° and 120°). In the experiments, an R probe with a tip diameter of 11 μm was used.

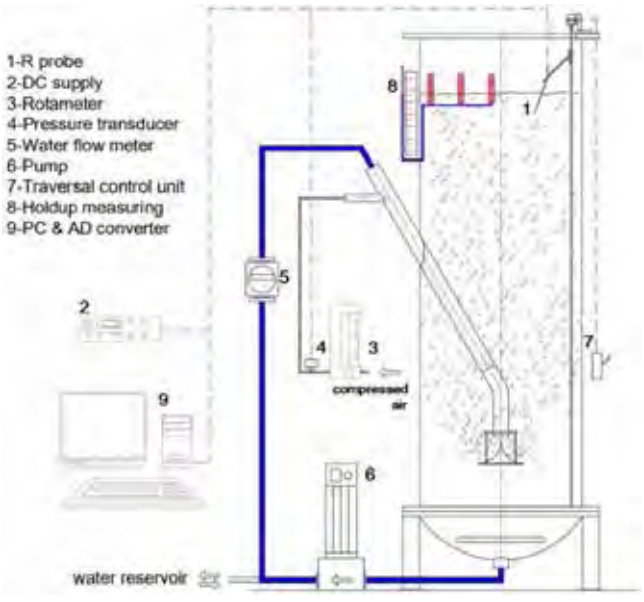


***Figure 2 :*** *Experimental setup.*

The voltage response from the R probe corresponds to the structural function $M_p$, defined as:

$$M_p(x,t) = \begin{cases} 1, & x \text{ is occupied by } p \\ 0, & x \text{ is not occupied by } p \end{cases} \qquad p = \{l, g, S\} \quad (3)$$

where three states of the phase $p$ are possible in a two-phase flow field, at a particular point $x$ at any time $t$, $l$ is the liquid phase, $g$ is the gas phase, and $S$ is the phase interface. The structural function $M_p$ was discriminated into a binary signal from which the LVF was calculated:

$$\alpha(x) = \lim_{\Delta T\to\infty}\frac{\sum_i \Delta t_{gi}}{\Delta T} \quad (4)$$

where $\Delta T$ denotes the total sampling time and $\Delta t_{Gi}$ the gas-phase residence time. A very stable procedure with a single threshold at 6% of the signal amplitude was used here as the phase-discrimination procedure. The R probe was powered by a DC supply, and the maximum response magnitude due to the phase change was of 2.3 V. A 12-bit A/D Lab-PC card (National Instruments, NI) supported by LabView software (NI) was used to acquire and store the data. The sampling rate and duration were set to 5 kHz and 3 min, respectively, for each LVF measurement. For each hydrodynamic regime the LVF was evaluated at 342 node locations in the vertical half-section plane of the column. Based on our visual observation, no coalescence or even break-up kernels could be detected, as can be seen in *Fig. 3*. At the deflector level, photographs were taken to estimate the range of bubble sizes, which was between 2.5 and 3.2 mm. According to the very small bubbles generated by the static mixer in our case, all three regimes could be classified as homogeneous flow regimes. Due to the fact that all the intension was oriented towards measurements of the LVF distribution, no further measurements of bubble size were made.

## 3 Results and discussion

### 3.1 Void-fraction distribution

Combining the air and water flow rates, three basic hydrodynamic regimes, for which the photographs are presented in *Fig. 3*, were studied in detail:

a) w3a5 - water: 0.8318 kg/s and air: 0.00248 kg/s
b) w6a5 - water: 1.6637 kg/s and air: 0.00248 kg/s
c) w9a10 - water: 2.4955 kg/s and air: 0.00523 kg/s

In our case the two-phase flow is generated by mixing water and air in the static mixer, which ended just above the deflector (see the detail in Fig.1). The entering two-phase flow causes strong liquid circulation in both sections (upper and lower) of the column. In

the upper section, rising bubbles in the middle of the column cause an upward liquid flow, which turns just below the liquid surface, radially towards the column wall and then downward, close to the column wall. The water exits the column in the lower section, below the deflector and the safety plate at the bottom (where the safety plate prevents even single bubbles from entering the outlet). This hydrodynamic regime cannot be compared to, for example, any concurrent or countercurrent flow regime of a *conventional* bubble column. Generally, in a bisectional bubble column, three different regions can be distinguished:

(R1) the entering two-phase flow coming downwards from the static mixer is deflected symmetrically and discharged radially towards the vessel walls (causing strong liquid circulation in both the upper and lower sections of the column),
(R2) the region of dispersed bubbles moving upwards due to buoyancy,
(R3) the region of liquid only, without any trapped bubbles.

The selected measurement grid and procedures allowed us to plot the void-fraction gradients in very fine steps, while only selected contours of a constant LVF are plotted for better clarity (from 0.5–2% with a 0.5% step and from 1–10% with a 1% step), as can be seen in Fig. 4. In the least-intense regime w3a5, the liquid discharge flow was rather weak, and consequently all the discharge two-phase flow in the R1 region redirected upwards to the free surface due to buoyancy. As can be seen from the visual observations and the contours of α=constant in Fig.4, the rising bubbles were relatively uniformly distributed with the LVF in the range of 1% and 3% around the middle of the column. Following the lower LVF, i.e., 0.5%, it can be seen that the bubbles spread within the vessel with the height. Below the deflector and above, close to the vessel wall, until half of the liquid column, the two-phase circulation in the liquid bulk was not established. In this regime, the volume-integrated value $\alpha_v$ of the LVF was found to be 0.84%. Increasing the water flow rate (w6a5 regime) led to a small recirculation of the two-phase mixture, which was observed just below the deflector edge. The dispersed air reached deeper regions below the deflector Spreading, rising bubbles were seen over a wider area, achieving voidances between 1% and 3%, concentrically. The overall integrated void fraction increased by almost 50%, compared to the previous regime, to 1.24%. In the last hydrodynamic regime (w9a10), both media increased. This caused a very intense recirculation of the two-phase flow just below the deflector. The voidage increased from very low close to the vessel wall up to 8% in the middle of the column. This airflow enlargement is reflected in the increased value of $\alpha_v$, which is now ~2.8 times higher than for previous regimes, and equals 3.47%. The region of liquid (R3) shrank to just the area below the deflector, where only liquid was still provided to the pump.

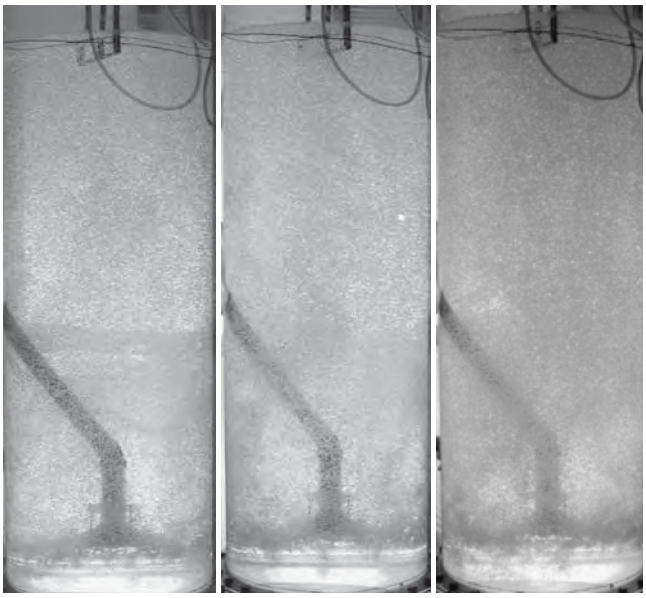

***Figure 3 :*** *Photographs of the hydrodynamic regimes: from left w3a5, w6a5, and w9a10.*

Generally, in all the studied cases most of the gas was concentrated in the middle of the column, just above the deflector.

## 3.2 Radially integrated void fraction

The radially integrated values of α are defined as:

$$\alpha_r(z) = \frac{2}{R^2}\int_0^R \alpha_r(r,z)\cdot r\cdot \mathrm{d}r \qquad (5)$$

and are shown in Fig.5. To facilitate comparison of void fraction with the Fig. 4, the $\alpha_r(z)$ is displayed on the *x* axis. Two typical features can be seen in Fig.5, i.e., the characteristic void peak caused by the deflector and the increasing of $\alpha_r$ with the height. In the w9a10 regime, the strong inertia of the two-phase flow caused the void peak just below the deflector at ~290 mm, which corresponds to the recirculation flow. In the w6a3 regime the peak shifts to a height of 330 mm due to a weaker discharge flow, as can be seen by the recirculation contours shown in *Fig.4*. In the w3a5 regime, a weak peak occurred, probably due to the weak two-phase discharge causing no recirculation.

## 3.3 Comparison between the integrated volume and the global void fraction

The results of the volume-integrated values:

$$\alpha_V = \int \alpha_r(h)\cdot \mathrm{d}h \qquad (6)$$

for the regimes discussed above are shown in Table 1 and compared with the measured gas holdups ac-

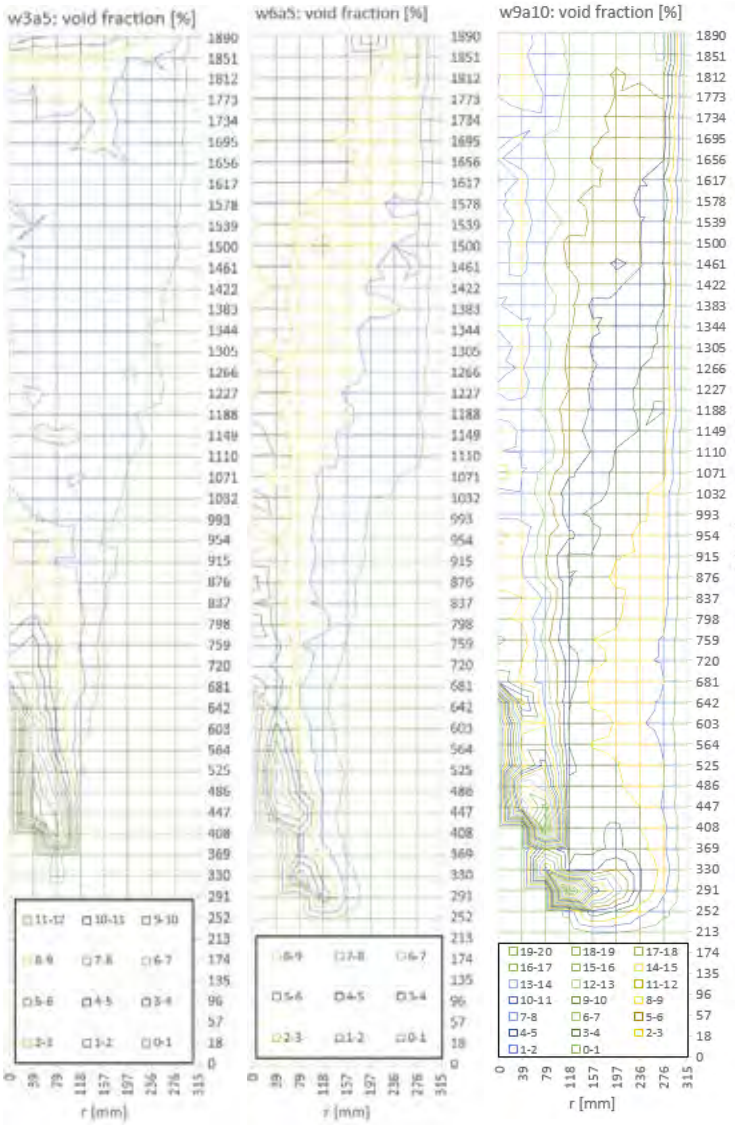


***Figure 4 :*** *Interpolated areas of the LVF.*

cording to Eq.2. Significantly higher $\alpha_G$ and $\alpha_v$ were achieved in the regime w9a10 compared to w3a5 and w6a5.

***Table 1 :*** *Volume-integrated void fractions compared with the measured gas holdup*

| | w3a5 | w6a5 | w9a10 |
|---|---|---|---|
| $\alpha_v$, % | 0.84 | 1.24 | 3.47 |
| $\alpha_G$ , % | 0.79±0.05 | 1.38±0.05 | 3.58±0.07 |
| $\varepsilon = (\alpha_v - \alpha_G)/\alpha_G$ | 0.063 | -0.101 | -0.031 |

Generally, small differences in the relative error ***ε*** found within the limits between 6.3% and -10.1% confirm the applicability of the entire experimental method, which is based on the local detection of the void fraction (using an R probe and the corresponding discrimination method) in such nonhomogeneous two-phase systems.

## 4 Conclusions

The local void fraction (LVF) in a bisectional bubble-column reactor was measured in the vertical *r–z* half-plane of the column at 342 grid nodes using an R probe and the appropriate discrimination procedure.

The use of the R probe in a bi-sectional bubble column was reasonable because of the wide impact angle. The node values, as data matrices, can be used (in future work) as useful tools to check the CFD predictions.

The tendency of the bubbles to concentrate in the middle of the column above the deflector could be observed in all the regimes.

To the best of our knowledge, this is the first time that local void fractions were measured and compared with the gas holdup in such a pilot-scale bubble column.

Based on the radially integrated values, characteristic void peaking can be observed (at different heights under specific regimes), which was just above the deflector height as well as the increasing of $\alpha_r$ with the height. A comparison of the measured gas holdups with the volume-integrated LVF showed small differences between them and confirmed the applicability of the entire experiment as

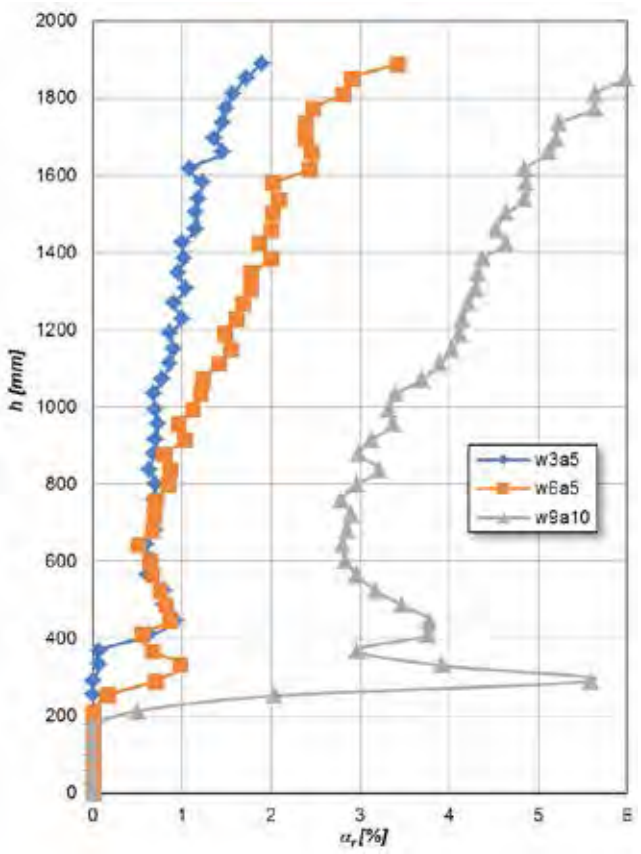


***Slika 5 :*** *Radially integrated values of local void fraction as a function of height.*

well as the reliability of the LVF in such nonhomogeneous, two-phase systems.

## References


[1] J. Levec, Arrangement and process for oxidizing an aqueous medium. US Patent No. 5,928,521, US Patent No. 5,928,521, 1999.

[2] J. Levec, A. Pintar, Catalytic wet-air oxidation processes: A review, Catal. Today. 124 (2007) 172–184. doi:10.1016/j.cattod.2007.03.035.

[3] E. Krepper, B.N. Reddy Vanga, A. Zaruba, H.M. Prasser, M.A. Lopez de Bertodano, Experimental and numerical studies of void fraction distribution in rectangular bubble columns, Nucl. Eng. Des. 237 (2007) 399–408. doi:10.1016/j.nucengdes.2006.07.009.

[4] A. Busciglio, F. Grisafi, F. Scargiali, A. Brucato, On the measurement of local gas hold-up and interfacial area in gas-liquid contactors via light sheet and image analysis, Chem. Eng. Sci. 65 (2010) 3699–3708. doi:10.1016/j.ces.2010.03.004.

[5] A. Bombač, I. Žun, B. Filipič, M. Žumer, B. Filipic, M. Žumer, Gas-Filled Cavity Structures and Local Void Fraction Distribution in Aerated Stirred Vessel, AIChE J. 43 (1997) 2921–2931. doi:10.1002/aic.690431105.

[6] I. Žun, M. Perpar, B. Filipič, Probe Measurements of Local Carrying Gas Fraction in Trickle-Bed Reactor, Exp. Therm. Fluid Sci. 15 (1997) 163–173.

[7] M. V. Sardeshpande, S. Harinarayan, V. V. Ranade, Void fraction measurement using electrical capacitance tomography and high speed photography, Chem. Eng. Res. Des. 94 (2015) 1–11. doi:10.1016/j.cherd.2014.11.013.

[8] J.P. Schlegel, S. Miwa, M. Griffiths, T. Hibiki, M. Ishii, Development of impedance void meter for evaluation of flow symmetry, Ann. Nucl. Energy. 63 (2014) 525–532. doi:10.1016/j.anucene.2013.08.026.

[9] Y. Nagase, H. Yasui, T. Sumimoto, A method for simultaneous measurements of size, shape, direction of motion and speed of ellipsoidal bubbles, Kagaku Kogaku Ronbunshu. 7 (1981) 532–537.

[10] M. Barigou, M. Greaves, Bubble-Size Distributions Gas-Liquid in a Mechanically, Chem. Eng. Sci. 47 (1992) 2009–2025.

[11] S.S. Alves, C.I. Maia, J.M.T. Vasconcelos, A.J. Serralheiro, Bubble size in aerated stirred tanks, Chem. Eng. J. 89 (2002) 109–117. doi:10.1016/S1385-8947(02)00008-6.

[12] I. Žun, B. Filipič, M. Perpar, A. Bombač, Phase discrimination in void fraction measurements via genetic algorithms, Rev. Sci. Instrum. 66 (1995) 5055–5064.

[13] S. Ojima, K. Hayashi, S. Hosokawa, A. Tomiyama, Distributions of void fraction and liquid velocity in air-water bubble column, Int. J. Multiph. Flow. 67 (2014) 111–121. doi:10.1016/j.ijmultiphaseflow.2014.05.008.

[14] A. Bombač, I. Žun, Gas-filled cavity structures and local void fraction distribution in vessel with dual-impellers, Chem. Eng. Sci. 55 (2000) 2995–3001. doi:10.1016/S0009-2509(99)00469-8.

[15] J.P. Schlegel, T. Hibiki, M. Ishii, Characteristics of two-phase flows in large diameter channels, Nucl. Eng. Des. 310 (2016) 544–551. doi:10.1016/j.nucengdes.2016.10.047.

[16] A. Bombač, I. Žun, Individual impeller flooding in aerated vessel stirred by multiple-Rushton impellers, Chem. Eng. J. 116 (2006) 85–95. doi:10.1016/J.CEJ.2005.10.009.

[17] A. Bombač, M. Žumer, I. Žun, Power consumption in mixing and aerating of shear thinning fluid in a stirred vessel, Chem. Biochem. Eng. Q. 21 (2007) 131–138.


## Eksperimentalna študija porazdelitve deleža plinaste faze v dvodelni koloni z mehurčki


**Povzetek:**

V prispevku je prikazana porazdelitev lokalnega deleža plinaste faze (LVF) v pilotni dvodelni koloni z mehurčki premera 0,63 m, kjer je bilo izvedeno mešanje zraka in vode s statičnim mešalom. Zaradi pomanjkanja tovrstnih podatkov v literaturi je bil LVF izmerjen na 342 vozliščih v navpični polovični ravnini kolone. Z lokalno detekcijo faz v določeni točki s pomočjo uporovne sondo in nadaljnjim postopkom fazne diskriminacije sondnega signala smo omogočili kvantitativno vrednotenje faz v pilotni koloni z mehurčki. Majhne razlike med volumsko integriranimi vrednostmi LVF in izmerjenimi globalnimi prirastki plinaste faze, temelječimi na spremembah višine gladine, so pokazale dobro ujemanje v vseh obravnavanih režimih.



**Ključne besede:**

dvodelna kolona z mehurčki, uporovna sonda, lokalni delež plinaste faze, volumski delež plinaste faze, prirastek plinaste faze



### Acknowledgments

This experimental study was conducted under Contract No. P2-0162 by the Slovenian Ministry of Higher Education and Science.